PHYSICAL REVIEW

LETTERS

VOLUME 61 | 10 OCTOBER 1988 | NUMBER 15

Nonchaotic Transition from Quasiperiodicity to Complete Phase Locking

Preben Alstrøm

Center for Polymer Studies, Boston University, 590 Commonwealth Avenue, Boston, Massachusetts 02215

and

Bo Christiansen and Mogens T. Levinsen

Physics Laboratory, H. C. Ørsted Institutet, Universitetsparken 5, DK-2100 Copenhagen Ø, Denmark

(Received 7 March 1988)

We show the existence of a generic integrate-and-fire phenomenon which separates the transition to complete phase locking from the transition to chaos. We argue that our picture provides a natural explanation of "missing" hysteretic bands in the Belousov-Zhabotinskii reaction. In addition, we explain the origin of experimentally observed "deviations from universality" and bumps in the Arnold tongues in driven relaxation oscillators.

PACS numbers: 05.45.+b, 82.20.Mj, 84.30.−r, 87.10.+e

Recently, much attention has been devoted to systems showing the occurrence of entire nonchaotic regions with complete phase locking. Such regions are observed in a wide range of biological[1,2] and chemical[3,4] systems, including neuronal encoding[2] and the Belousov-Zhabotinskii reaction.[4] Also, Cumming and Linsay,[5] studying a driven relaxation oscillator, have presented experimental results which suggest deviations from universality in the transition to chaos. They have determined the position of several phase-locked regions (Arnold tongues), each characterized by a certain rational rotation number, i.e., ratio between oscillator and drive frequency. Some of these tongues are shown in Fig. 1. A critical line is defined, below which no chaotic behavior is present in the Poincaré map (Fig. 2). Along this line (solid line in Fig. 1) the dimension D of the quasiperiodic set is computed to be $D=0.795$ which is compared to the dimension $D=0.87$ obtained from iterations of ordinary circle maps at criticality.[6] This dimensionality has been predicted and found to characterize the quasiperiodic set at the transition to chaos in a class of nonlinear phase-locking systems.[6,7] Cumming and Linsay find the line associated with the dimension $D=0.87$ (dashed line in Fig. 1) well below the transition to chaos.

In this Letter we give analytical evidence for a *new* type of transition from quasiperiodicity to complete phase locking with no chaos involved. This transition is a consequence of a generic integrate-and-fire phenomenon and manifests itself as a critical line along which a gap in the Poincaré map emerges. Below and at criticality the phase diagram exhibits an ordinary circle-map phase diagram, for example, a dimension $D=0.87$ of the quasiperiodic set at the critical line. Above this line the phase locking is complete, however, no chaos will occur before a zero-slope inflection point develops in the Poincaré map. Universal scaling properties normally characterizing the transition to chaos will be suppressed as a result of the preceding critical transition, as we shall see. In particular, the dimension $D=0.795$ (Ref. 5) is nonuniversal and a result of the presence of the steep part in the Poincaré map (Fig. 2). Moreover, our picture explains why bumps are present in the Arnold tongues (Fig. 1).

To understand the basic idea, we consider a simple driven relaxation oscillator where the voltage builds up from a lower threshold $T_0=0$ to a firing threshold $T_1=1$ following a standard exponential curve,

$$\dot{V}=-\Gamma V+I. \tag{1}$$

When $I>\Gamma$, oscillations develop since the voltage

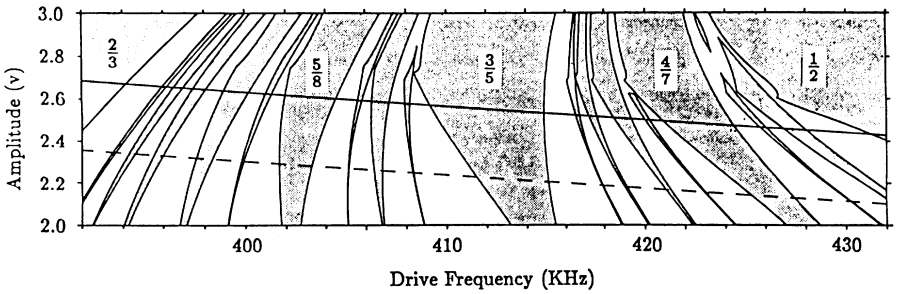

FIG. 1. Phase diagram of the driven relaxation oscillator studied by Cumming and Linsay (Ref. 5). The rationals in the phase-locked regions (shaded) are associated rotation numbers. The solid and the dashed lines are explained in the text.

reaches unity and firing takes place resetting the voltage to zero. We want to study the consequences when this integrate-and-fire system is driven by a sine wave $U(t)=A\sin(2\pi t)$. This modulation can be imposed on the lower threshold, on the upper threshold, or on the input current. Hence, aside from Eq. (1) the system is described by the condition

$$V(t)=t\rightarrow V(t^+)=U(t) \tag{2a}$$

for the lower threshold modulation, and by the condition

$$V(t)=1+U(t)\rightarrow V(t^+)=0 \tag{2b}$$

for the upper threshold modulation. For the current modulation, $U(t)$ is added to the right-hand side of Eq. (1), leaving the initial firing condition,

$$V(t)=1\rightarrow V(t^+)=0. \tag{2c}$$

In order to describe the phase-locking structure, we determine the functional relation between two consecutive firing times, $\tau_{m+1}=f(\tau_m)$. However, since the Poincaré map plays a central role in understanding the transition to chaos and the transition to complete phase locking, we first elaborate on the connection between f and the Poincaré map. It is known that if this map is monotonic, the rotation number is uniquely defined (in this sense there is no chaos); moreover if the map is (sufficiently) smooth, quasiperiodicity has positive measure (i.e., no complete phase locking). To use these results on scaling, it is important to relate the firing function to the Poincaré map, in order to conclude what the behavior of phase-locking structure is from the behavior of the firing function. This relation is given below.

The one dimensionality of the Poincaré map relies on the fact that the time evolution of the voltage $V(t)$ after transients have died away is described by one integration constant. We take here the integration constant to be a firing time τ. This defines a function $V_\tau(t)$ as the solution to Eq. (1), choosing $V_\tau(\tau)=1$ for the lower threshold modulation and $V_\tau(\tau)=0$ for the upper threshold and the current modulation. Now we define the function g by (Fig. 3)

$$g(\tau)=V_{\tau+n}(n), \tag{3}$$

where the periodicity of the solution assures that g is independent of n, n being an integer. The periodicity also assures that the firing function is a circle map, i.e., $f(t+1)=f(t)+1$. We can now write down the relation between the firing function f and the Poincaré map h, which here is defined as the function $V(n)\rightarrow V(n+1)$

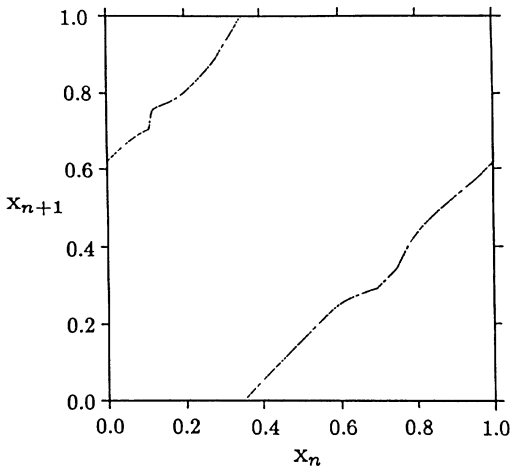

FIG. 2. Poincaré map obtained at the transition to chaos for the driven relaxation oscillator studied by Cumming and Linsay (Ref. 5).

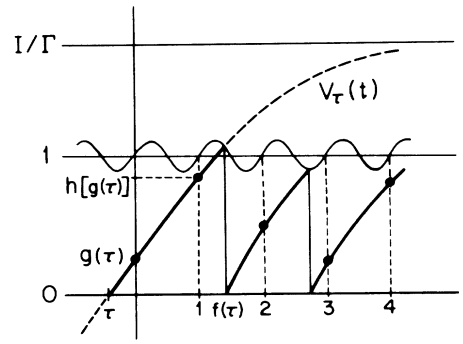

FIG. 3. Illustration showing how $g(\tau)$ is defined for upper threshold modulation.

(see Fig. 3),

$$h(x)=\begin{cases} g[f^{k}(g^{-1}(x))-1], & \text{if } 0\le x\le x^{*}, \\ g[f^{k+1}(g^{-1}(x))-1], & \text{if } x^{*}<x\le 1. \end{cases} \quad (4)$$

Here, $k=[R]$ denotes the integral value of the rotation number R. The Poincaré map consists of two parts with $h(0)=h(1)$, and x^{*} defined by $h(x^{*})=1$ $[h(x^{*+})=0]$. The two forms of $h(x)$ correspond to having k or $k+1$ firings between time n and $n+1$. In Eq. (4) we have assumed that g is invertible. If the rotation number R is rational, $R=P/Q$, the relation between h and f, Eq. (4), shows that a stable q cycle $[x_0, x_1=h(x_0), \ldots, x_{Q-1}=h(x_{Q-2})]$ for h maps onto a stable P cycle $[y_0=g^{-1}(x_0), y_1=f(y_0), \ldots, y_{P-1}=f(y_{P-2})]$ for f. Thus, when g has a nonzero slope everywhere, the phase-locking structure is determined by the circle-map dynamics of f by inversion of rotation number (this has no influence on the scaling properties at criticality as regards dimension, decay exponents at the golden mean, etc.

We now return to our simple driven relaxation oscillator. For the threshold modulations we find that

$$g(\tau)=[I-(I-\theta\Gamma)e^{\Gamma\tau}]/\Gamma, \quad (5)$$

where $\theta=1$ for lower threshold and $\theta=0$ for upper threshold modulation. We notice that this function has negative slope for all τ (hence, g is invertible). Thus, the system is characterized by the behavior of the firing function f. For the lower threshold f is given by

$$f(\tau)=\tau+g^{-1}(U(\tau)). \quad (6)$$

This is a smooth monotonic circle map below the critical line $A=I(4\pi^2+\Gamma^2)^{1/2}$, along which f has a zero-slope inflection point. We conclude that pure lower threshold modulation reveals ordinary circle-map dynamics, including scaling and a transition chaos at criticality.

The situation turns out to be quite different for the upper threshold modulation. Now it is the inverse of the firing function f which has a simple expression,

$$f^{-1}(\tau)=\tau+g^{-1}(1+U(t)). \quad (7)$$

This expression is of course only valid when the right-hand side of Eq. (7) is monotonic, which is the case below and at the critical line $A=(I-\Gamma)/(4\pi^2+\Gamma^2)^{1/2}$ where f^{-1} has a zero-slope inflection point. At positive damping we notice that, increasing the amplitude, this line is reached *before* the transition to chaos caused by a lower threshold modulation. In all, f^{-1} obeys ordinary circle-map dynamics (including scale) below and at criticality, and this is therefore also true for f.[8] *At this point we emphasize that this criticality gives no occasion for a transition to chaos.* Contrary to the lower threshold modulation, here some of the threshold becomes "invisible" for the signal as illustrated in Fig. 4. This leads to a gap in the firing function f and in the Poincaré map h.

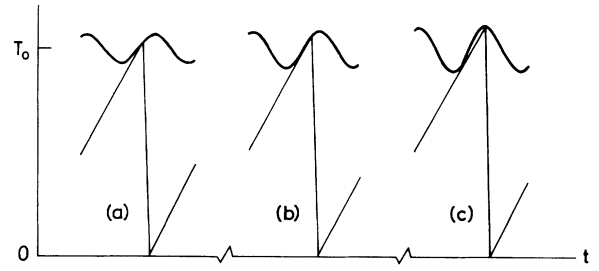

FIG. 4. Time evolution of the voltage V and the threshold $T=1+U$. (a) Below criticality: the slope $\dot{V}$ at each firing is larger than $\dot{T}$. (b) At criticality: a firing point develops where $\dot{V}=\dot{T}$. (c) Above criticality: certain parts of the threshold can not contain firing points.

They are, however, still monotonic, and hence, the rotation number is independent of initial conditions.[9] Above criticality, where a gap is present, the generic behavior at the borders of the gap is square-root-like on one side [corresponding to coming from the left in Fig. 4(c)] and linear from the other side (from which the firing time jumps abruptly). This is exactly what is observed in Fig. 2, disregarding the smoothness of the real flow which imposes a finite (but steep) slope.

From the "cutting" effect by which the visible part of the threshold shrinks, the origin of bumps in the Arnold tongues (Fig. 1) also becomes obvious. The tongues determined by Eq. (7) are cut by the visibility condition (i.e., the cycle points have to be visible for the signal), leaving a bump on one side of the tongues. As regards the quasiperiodic set we know that a discontinuity implies that the measure of this set is zero,[9] i.e., that the phase locking is complete, and calculations show that the set has dimension zero.[10] However, at a gap size Δ the stability intervals decay exponentially as $(1-\Delta)^{Q}$. This means that the dimension decays toward zero as $D\sim(\ln Q)/Q\Delta$, which is a very slow convergence, and the zero dimensionality will therefore hardly be obtained from an experiment. *The dimension $D=0.795$ is a mere result of an arbitrary gap size in the Poincaré map and has no special relation to the transition chaos. The true dimensionality at this transition is zero, arising from a preceding criticality.* The smoothness of a real flow, will, however, remove this criticality, leaving an ordinary circle-map scaling. On the other hand, this scaling structure is in practice not perceivable. Regarding the actual experimental value $D=0.795$, we refer the reader to studies on circle maps with higher-order inflection points.[10-12] From this analysis, which confirms that zero dimensionality due to a small gap is approached very slowly, we can understand why a dimension of size about 0.8 and not a dimension close to zero is obtained. Moreover, a change in order changes the golden-mean decay number[11,12] δ in accordance with the range in which Cumming and Linsay find their value of δ.

Finally, we discuss the current modulation. Solving

Eq. (1) with $U(t)$ added on the right-hand side yields

$$g(\tau) = -V_0(\tau)e^{\Gamma\tau}. \quad (8)$$

The function g is monotonic only below the critical line $A=I$, determined by $g''(\tau)=g'(\tau)=0$, where the signal has zero slope somewhere at the lower threshold. Along this line g gives occasion for an ordinary transition to chaos. However, this transition is again preceded (at smaller amplitudes) by another criticality related to the firing function. We get

$$f^{-1}(\tau) = g^{-1}(g(\tau)+e^{\Gamma\tau}), \quad (9)$$

which is valid to the point where the right-hand side becomes noninvertible. This happens when $g''(\tau) = \Gamma g'(\tau) = -\Gamma^2 e^{\Gamma\tau}$, giving the critical line $A=I-\Gamma$. Along this line the signal attains zero slope somewhere at the upper threshold, while above the signal becomes nonmonotonic, leaving a gap in the firing function and in the Poincaré map. Thus, the current modulation separates the transition to complete phase locking and the transition to chaos. At the first transition the quasiperiodic set has dimension $D=0.87$, while this is zero above. In particular, the ordinary circle-map scaling properties are suppressed at the transition to chaos.

We want to comment on the observation that the maximal slope of the Poincaré map in Fig. 2 is finite and not infinite. As already stated this is a consequence of the smooth behavior of the flow. The upper threshold corresponds to a region in phase space where trajectories greatly separate over short times to be attracted to an unstable focus corresponding to the lower threshold. The (positive) real part of the eigenvalue is small here compared to the contracting eigenvalue which determines the resetting time. In this sense the attractor is a typical Rössler- or Lorenz-type attractor.[13] Such a behavior has recently been suggested also to characterize chemical systems such as the Belousov-Zhabotinskii reaction.[14] Without writing down any complicated flow equation our picture provides a simple understanding to why an entire nonchaotic but complete phase-locked region is obtained experimentally.[4]

In conclusion, we have shown that the generic properties of driven relaxation oscillators can be understood from a simple integrate-and-fire principle. This introduces a critical transition to complete phase locking which precedes the transition to chaos, it explains the scaling properties, and spells out the general behavior of the Arnold tongues, including the origin of bumps thereon. As regards the connection to circle maps, previous studies on ordinary circle maps and circle maps with a discontinuity are sufficient to describe the scaling structure. We believe that our picture is applicable to many mode-locking systems characterized by a local region where the flow greatly separates.

We would like to thank Dwight Barkley and Predrag Cvitanović for stimulating and useful discussions. One of us (P.A.) wishes to thank Professor Harry Swinney and The University of Texas Physics Department at Austin for kind hospitality which made these discussions possible. The Center for Polymer Studies is supported by grants from the National Science Foundation and the U.S. Office of Naval Research. This work has also been supported by the Danish Natural Science Research Council.

[1]L. D. Harmon, Kybernetik **1**, 89 (1961); L. Glass and M. C. Mackey, J. Math. Biol. **7**, 339 (1979).

[2]J. F. Fohlmeister, Kybernetik **13**, 104 (1973); J. P. Keener, F. C. Hoppensteadt, and J. Rinzel, SIAM J. Appl. Math. **41**, 503 (1981).

[3]J. Chopin-Duman, C. R. Acad. Sci. (Ser.) C **287**, 553 (1978); M. Alamgir and I. R. Epstein, J. Am. Chem. Soc. **105**, 2500 (1983).

[4]J. Maselko and H. L. Swinney, J. Chem. Phys. **85**, 6430 (1986).

[5]A. Cumming and P. S. Linsay, Phys. Rev. Lett. **59**, 1633 (1987).

[6]M. H. Jensen, P. Bak, and T. Bohr, Phys. Rev. A **30**, 1960 (1984).

[7]P. Alstrøm and M. T. Levinsen, Phys. Rev. B **31**, 2753 (1985), and **32**, 1503 (1985).

[8]For rational rotation number R, every $-R$ cycle for f^{-1} maps onto an R cycle for f; for R irrational, the conjugacy to the pure rotation $\tau \to \tau - R$ for f^{-1} gives a conjugacy to the inverse rotation $\tau \to \tau + R$ for f.

[9]J. P. Keener, Trans. Am. Math. Soc. **261**, 589 (1980).

[10]P. Alstrøm, Commun. Math. Phys. **104**, 581 (1986).

[11]P. Alstrøm, M. T. Levinsen, and D. R. Rasmussen, Physica (Amsterdam) **26D**, 336 (1987).

[12]S. Shenker, Physica (Amsterdam) **5D**, 405 (1982).

[13]O. E. Rössler, Phys. Lett. **57A**, 397 (1976); E. Lorenz, J. Atmos. Sci. **20**, 130 (1963).

[14]D. Barkley, to be published.

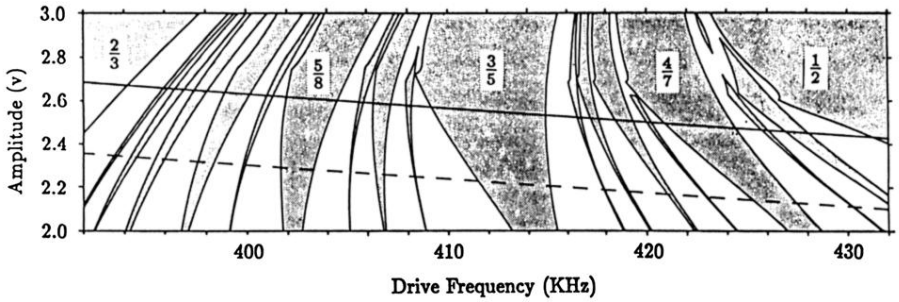

FIG. 1. Phase diagram of the driven relaxation oscillator studied by Cumming and Linsay (Ref. 5). The rationals in the phase-locked regions (shaded) are associated rotation numbers. The solid and the dashed lines are explained in the text.